EPR and FTIR studies reveal the importance of highly ordered sterol-enriched membrane domains for ostreolysin activity

Katja Rebolj [a], Biserka Bakrač [a], Maja Garvas [b], Katja Ota [a], Marjeta Šentjurc [b], Cristina Potrich [c,d], Manuela Coraiola [c,d], Rossella Tomazzolli [c,d], Mauro Dalla Serra [c,d], Peter Maček [a], Kristina Sepčić [a,*]

[a] *Department of Biology, Biotechnical Faculty, University of Ljubljana, Večna pot 111, 1000 Ljubljana, Slovenia*
[b] *EPR Center, J. Stefan Institute, Jamova 39, 1000 Ljubljana, Slovenia*
[c] *CNR—Institute of Biophysics, via alla Cascata 56/C, 38123 Trento Povo, Italy*
[d] *Bruno Kessler Foundation, via Sommarive 18, 38123 Trento Povo, Italy*

ARTICLE INFO

ABSTRACT

Ostreolysin is a cytolytic protein from the edible oyster mushroom (*Pleurotus ostreatus*), which recognizes specifically and binds to raft-like sterol-enriched membrane domains that exist in the liquid-ordered phase. Its binding can be abolished by micromolar concentrations of lysophospholipids and fatty acids. The membrane activity of ostreolysin, however, does not completely correlate with the ability of a certain sterol to induce the formation of a liquid-ordered phase, suggesting that the protein requires an additional structural organization of the membrane to exert its activity. The aim of this study was to further characterize the lipid membranes that facilitate ostreolysin binding by analyzing their lipid phase domain structure. Fourier-transformed infrared spectroscopy (FTIR) and electron paramagnetic resonance (EPR) were used to analyze the ordering and dynamics of membrane lipids and the membrane domain structure of a series of unilamellar liposomes prepared by systematically changing the lipid components and their ratios. Our results corroborate the earlier conclusion that the average membrane fluidity of ostreolysin-susceptible liposomes alone cannot account for the membrane activity of the protein. Combined with previous data computer-aided interpretation of EPR spectra strongly suggests that chemical properties of membrane constituents, their specific distribution, and physical characteristics of membrane nanodomains, resulting from the presence of sterol and sphingomyelin (or a highly ordered phospholipid, dipalmitoylphosphatidylcholine), are essential prerequisites for ostreolysin membrane binding and pore-formation.

© 2010 Elsevier B.V. All rights reserved.

1. Introduction

Ostreolysin is a cytolytic protein from the oyster mushroom (*Pleurotus ostreatus*) [1]. For ostreolysin to bind and form pores in the lipid membrane, a specific combination of cholesterol and sphingomyelin is required, and its membrane activity is displayed only above 30 mol.% of membrane cholesterol [2,3]. Binding, and consequently pore-formation, can be diminished or abolished (i) by the addition of mono- or di-unsaturated phosphatidylcholine [2], (ii) by replacing cholesterol with other natural sterols or cholesterol derivatives [3], and (iii) by the addition of micromolar concentrations of fatty acids and lysophospholipids [4,5], as summarized in Fig. 1. These data suggest that ostreolysin interacts specifically with either cholesterol/sphingomyelin-enriched model membranes, in which lipids exist in the liquid-ordered (l_o) phase, or with specific membrane nano-, and micro-

assemblies such as lipid rafts (see rev. [6]). Indeed, immunostaining has shown selective binding and spotting of the protein on cell membranes, pointing to its association with distinctive membrane microdomains [7]. The latter were found to be sensitive to cholesterol depletion, but different from those that bind established raft-binding markers like caveolin and cholera toxin B subunit [5]. These findings are in agreement with a structural microheterogeneity of raft-like membrane structures, e.g. the coexistence of different lipid raft entities, which consequently display functional heterogeneity [6]. In order to further characterize differences between ostreolysin-susceptible and ostreolysin-resistant membranes, we have made a detailed comparative study of unilamellar liposomes with different lipid compositions and ratios of lipid components, using Fourier-transformed infrared spectroscopy (FTIR) and electron paramagnetic resonance (EPR).

FTIR provides information about the ordering of membrane lipids, by observing the absorbance band around 2850 cm^{-1} that is due to symmetric stretching vibrations of fatty acid methylene groups [8]. The position of this band is correlated to membrane fluidity, shifting towards higher wavenumbers with increasing temperature. Eventually, a broadening of the band can be observed, pointing to the decrease in
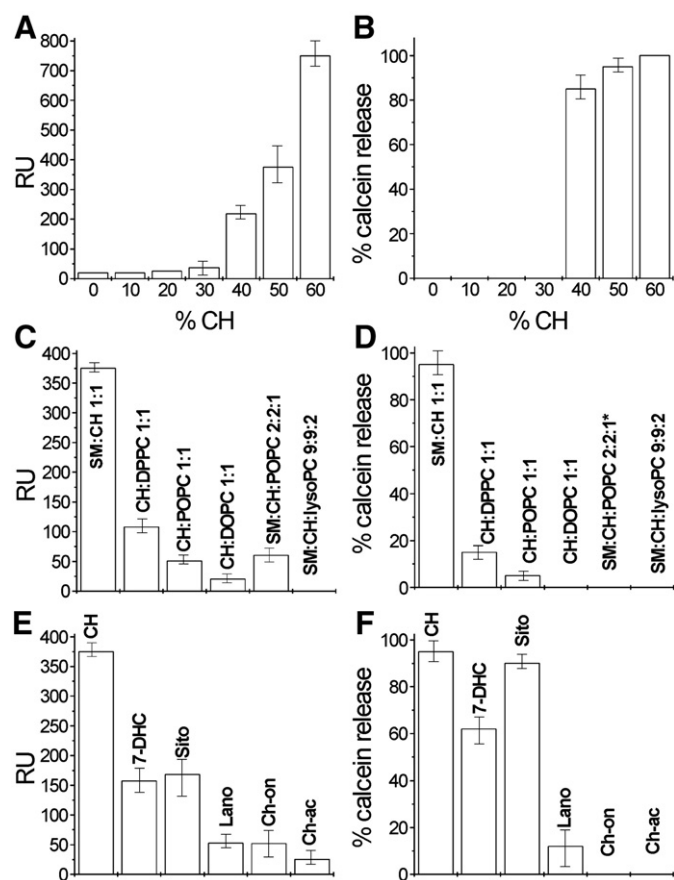
Fig. 1. The activity of ostreolysin as a function of the composition of lipid membranes analyzed in this study. Binding (left panels) of ostreolysin was assessed on lipid monolayers coupled to a Sensor Chip HPA using the surface plasmon resonance technique. The monolayers were composed of sphingomyelin and cholesterol in various molar ratios (A), mixtures of cholesterol and different phospholipids (C), or sphingomyelin and different steroids in a 1:1 molar ratio (E). The binding signal is expressed in resonance units (RU), corresponding to the response of bound ostreolysin after subtracting the fitted bulk component. Permeabilization (right panels) was studied spectrofluorimetrically by applying ostreolysin to calcein-loaded, sonicated unilamellar liposomes, and calculating the percentage of release of the fluorescent dye. Calcein-loaded liposomes were composed of sphingomyelin:cholesterol in various molar ratios (B), mixtures of cholesterol and different phospholipids (D), or sphingomyelin and different steroids in a 1:1 molar ratio (F). Each bar is a mean value of two independent measurements ± SEM. Lipid/protein ratios were 25 and 5.4 for binding and permeabilization studies. All the experiments were performed at 25 °C. CH = cholesterol, SM = sphingomyelin, 7-DHC = 7-dehydrocholesterol, Lano = lanosterol, Sito = sitosterol, CH-ac = cholesteryl acetate, CH-on = 5-cholesten-3-one, DPPC = dipalmitoylphosphatidylcholine, POPC = palmitoyl-oleoylphosphatidylcholine, DOPC = dioleoylphosphatidylcholine, lysoPC = palmitoyl-lysophosphytidiylcholine. *not determined. Adapted from [2,3].

ordering of membrane lipids. Saturated phospholipid chains usually have a frequency of the CH_2 stretch in the solid ordered (s_o) phase lower than 2850 cm^{-1}, while in the liquid disordered (l_d) phase the same vibrational band is close to 2853 cm^{-1} [8]. Besides information about the average ordering and dynamics of membrane lipids, further information about membrane domains can be obtained by EPR spectroscopy. For this purpose a lipophilic spin probe, which reflects the motional characteristics of its surrounding, has to be introduced into the liposome membrane. The line shape of the EPR spectra, which depends strongly on the motional mode of the spin probe, gives information on the ordering and dynamics of its local surroundings. Analysis of the spectra, taking into account the lateral membrane heterogeneity, provides information about the number, proportion and physical characteristics of coexisting membrane domain types [9–11]. In the present work, spin probes MeFASL(10,3) and MeFASL(2,11) were used, with the nitroxide group positioned on the 5th and 13th carbon

atoms respectively of the fatty acid alkyl chains. Thus, MeFASL(10,3) reports on the membrane fluidity characteristics close to the surface of the lipid bilayer, and MeFASL(2,11) on the properties of the hydrophobic bilayer core.

2. Materials and methods

2.1. Materials

Porcine brain sphingomyelin (SM), wool grease cholesterol (CH), 1,2-dioleoyl-sn-glycero-3-phosphocholine (DOPC), 1-palmitoyl-2-oleoyl-sn-glycero-3-phosphocholine (POPC), 1,2-dipalmitoyl-sn-glycero-3-phosphocholine (DPPC) and 1-palmitoyl-2-hydroxy-sn-glycero-3-phosphocholine (lysoPC) were from Avanti Polar Lipids (Alabaster, USA), β-sitosterol, lanosterol, and 7-dehydrocholesterol were from Sigma (St. Louis, USA), cholesteryl acetate from Fluka (Buchs, Switzerland), and 5-cholesten-3-one from Aldrich (St. Louis, USA). All lipids were of the highest grade of purity available, as stated by the producer. Prior to experiments, they were dissolved in chloroform or other organic solvents according to the manufacturers' instructions. The spin probes 5-doxylpalmitoyl- and 12-doxylpalmitoyl methyl ester (MeFASL(10,3) and MeFASL(2,11), respectively), were synthesized by S. Pečar (Faculty of Pharmacy, University of Ljubljana, Slovenia).

2.2. Methods

2.2.1. Preparation of sonicated liposomes

Lipid films were formed by removing the organic solvent from a lipid solution by rotary evaporation and vacuum drying. Lipids, at respective final concentrations of 10 or 20 mg/mL, were swollen in 10 mM HEPES pH 8.0 (for FTIR studies) or in liposome buffer, 140 mM NaCl, 20 mM Tris–HCl, pH 8.0 (for EPR measurements). They were vortexed vigorously to give multilamellar liposomes, which were further exposed to 8 cycles of freezing and thawing and sonicated using a 750 W Ultrasonic Processor (Cole Parmer, USA) as described [4]. After centrifugation (20 min, 16,000 ×g, 25 °C), the sonicated liposomes were incubated for 45 min at 40 °C and stored at 4 °C until use (up to 2 weeks). The exact lipid concentration of liposome suspensions was determined colorimetrically with Waco Free Cholesterol C and Wako test Phospholipids B (990-54009) kits (Waco Chemicals GmbH, Germany) two times (immediately after the preparation of liposomes, and again prior to FTIR or EPR measurements), and did not change with the time. Dimensions of liposomes were estimated by photon correlation spectroscopy with a Zeta Sizer instrument (Malvern Instruments, Worcestershire, U.K.) as reported [4]. These preparations give liposomes with diameters in the range of 80–120 nm, which remained in the same range after storage.

The following liposomes were prepared composed of (i) sphingomyelin and cholesterol in molar ratios ranging from 0 to 60% cholesterol, (ii) sphingomyelin, cholesterol and lysoPC in a molar ratio of 9:9:2, (iii) sphingomyelin with different natural or synthetic steroids (cholesterol, 7-dehydrocholesterol, lanosterol, β-sitosterol, cholesteryl acetate, and 5-cholesten-3-one) in 1:1 molar ratios, (iv) cholesterol and phosphatidylcholines (PCs) with different degrees of saturation (DOPC, POPC or DPPC) in 1:1 molar ratios, and (v) sphingomyelin, cholesterol and POPC in a 2:2:1 molar ratio.

2.2.2. FTIR measurements

Ordering and fluidity characteristics of liposomes over a temperature range from 5 to 90 °C were analyzed with FTIR using the Bio-Rad FTS 185 spectrometer (USA) with an MCT-detector. Samples were loaded in a liquid semi-permanent and thermostated cell (Specac, Woodstock USA) with CaF$_2$ windows separated by a 15 μm Teflon spacer. The sample compartment was purged continuously with nitrogen. Sixty-four scans between wavenumbers 600 and 4000 cm^{-1} were averaged at each temperature. Win-IR Pro 3.4 (DigiLab, USA) program was used for data

acquisition and analysis (i.e., background subtraction and identification of the peak at ~2850 cm^{-1} corresponding to the methylene symmetric stretching).

2.2.3. EPR measurements

Just prior to measurement, the liposomes prepared as described in Section 2.2.1 were sonicated again for 6–10 min, incubated at 45 °C for 30 min and centrifuged (5 min, 16,000×g, 25 °C). The liposomes in the supernatant were spin-labelled with MeFASL(10,3) or MeFASL(2,11) at a molar ratio of the spin probe to total lipids 1:250 in the following way [12]: a thin film of the spin probe was deposited on the walls of a glass tube by rotary evaporation of an ethanol solution of the spin probe. The liposome suspension was then placed into the tube and vortexed at room temperature for 10 min. The diameter of vesicles, determined as described in Section 2.2.1, did not change significantly after the spin-labeling procedure, and remained in the range of 80–120 nm. The samples (ca. 20 µl) were then transferred into glass capillary tubes for EPR measurements on an X-band EPR spectrometer Bruker ESP 300 in the temperature range relevant for physiological conditions from 4 °C to 39 °C, in 5 °C intervals. Spectrometer settings were: microwave power 10 mW, modulation amplitude 0.1 mT, and frequency of modulation 100 KHz. Seven scans were accumulated for each spectrum.

EPR spectra were analyzed with the computer program EPRSIM WIZ 6.2.2. (http://www.ijs.si/ijs/dept/epr). The program takes into account that the spectrum is composed of several spectral components reflecting different modes of restricted rotational motion of spin probe molecules in different membrane regions with different physical characteristics (solution, rafts, outer and inner layers, surrounding of proteins, etc.). Spectral components are described by different sets of spectral parameters: order parameter (S) ($S = 1$ for perfectly oriented molecules and $S = 0$ for isotropic motion of molecules); rotational correlation time (t_c), which describes the rate of motion; polarity correction factors of hyperfine splitting and g tensors (Pa and Pg), describing the differences in polarity of the spin probe surroundings; and a broadening constant (W) related primarily to unresolved hydrogen super-hyperfine interactions, contributions from other paramagnetic impurities (e.g. oxygen), and others [9]. From the best fit of calculated spectra to the experimental one, the spectral parameters of each spectral component are determined, as well as the relative proportion (d) of a particular spectral component. The latter is the relative amount of the spin probe with a particular motional mode and depends on the distribution of the spin probe between different membrane regions.

It should be stressed that the lateral motion of the spin probe within the membrane is slow on the time scale of the EPR spectra. Therefore each spectral component describes the properties of the spin probe's nearest surroundings on the nanometre scale and represents the sum of all membrane regions with the same properties. These membrane regions are referred to as types of membrane domains, with dimensions of the order of several nm. In other words, from the EPR point of view domains represent the group of molecules with similar ordering and dynamics irrespective to their location in the membrane. More small domains with the same physical characteristics could not be distinguished from few large domains. This also means that EPR does not reflect directly the macroscopic properties of membrane, like different phases (solid, liquid, and liquid crystal) but reflects the superstructure in the phases on a nm scale. For example, motional mode of lipids and consequently the spin probe in the vicinity of proteins, cholesterol etc. is different as at long range distance. Besides, some dynamic fluctuations within the phases can also be detected as a specific motional mode of spin probe. For that reason we use hereafter the term domain D types to distinguish them from domains observed by other techniques in model and cell membranes [6].

To obtain the best fit of a calculated EPR spectrum to the experimental one, the multi-run hybrid evolutionary optimization algorithm (HEO) [10] is used, together with a newly developed GHOST condensation procedure. HEO method is based on two basic optimization schemes: stochastic and population-based genetic algorithm which is good at finding promising regions in complex search space but may have difficulties in fine tuning and the deterministic and single-point optimization method (Simplex downhill) [9], which provides good results only if starting points are close to the solutions. Both methods are coupled together in HEO which is capable of fine tuning and requires no special starting points and no user intervention.

In order to get a reasonable characterization one still has to define the number of spectral components before applying the optimization. Besides, for each spectral component there are 5 independent parameters which should be fitted (S; t_c, W, Pa and d). Therefore it is possible that different combinations of parameters give good fit of calculated to the experimental spectra. To eliminate this problem the GHOST condensation procedure was developed [10]. According to this procedure, 200 independent HEO simulation runs for each EPR spectrum were applied, taking into account 4 different motional modes of the spin probe (23 spectral parameters). All the best fit sets of parameters obtained by 200 optimizations were evaluated according to the goodness of the fit (χ^2 filter) and according to the similarity of the parameter values of best fits (density filter). The parameters of the best fits were presented by three two-dimensional cross-section plots: (S–t_c, S–W, and S–Pa diagrams). The two other parameters of each diagram are defined by the intensities of the colors: red, green, and blue for t_c, W, and Pa (GHOST diagrams) [11]. These diagrams correspond to the groups of solutions that represent the motional modes of a spin probe in particular surroundings and describe the properties of different types of membrane domains (designated D1–D4). They give information about the number of different domain types on nanometer scale, the dynamics of motion, ordering, and about the polarity of the spin probe surroundings within each domain D type.

3. Results

3.1. FTIR measurements

3.1.1. FTIR analysis of sphingomyelin:cholesterol sonicated liposomes

The wavenumber of the symmetric CH$_2$ stretching band of liposomes composed of sphingomyelin and cholesterol was plotted versus temperature for different cholesterol/sphingomyelin ratios (Fig. 2A). Pure porcine brain sphingomyelin liposomes display a sharp temperature-dependent transition from the s_o to the l_d phase at around 37 °C, which is consistent with previously published data [3]. Increasing the cholesterol content to 60%, leads to gradual disappearance of the cooperative gel-to-liquid phase transition, which is a typical consequence of the effect of cholesterol on phospholipid bilayer [13,14]. This can also be observed by following the wavenumber shift from 5 to 90 °C, which decreased from 2.9 to 0.9 cm^{-1} with increasing cholesterol/sphingomyelin ratio (Fig. 2A, insert). The fact that vesicles containing more than 30% cholesterol show a linear increase in frequency with increasing temperature points to the complete absence of a phase transition, and suggests the steady formation of the intermediate l_o phase over the temperature range tested. These data are in agreement with the sphingomyelin/cholesterol phase diagrams that show the formation of the l_o phase above 30 mol.% of cholesterol, and the disappearance of $s_o + l_o$, and $l_o + l_d$ phase boundaries below and above the transition temperature of sphingomyelin [15,16].

3.1.2. FTIR analysis of equimolar sphingomyelin:steroid sonicated lipid vesicles

The ordering characteristics of liposomes composed of sphingomyelin and different natural (cholesterol, 7-dehydrocholesterol, lanosterol, and β-sitosterol) and synthetic (cholesteryl acetate and
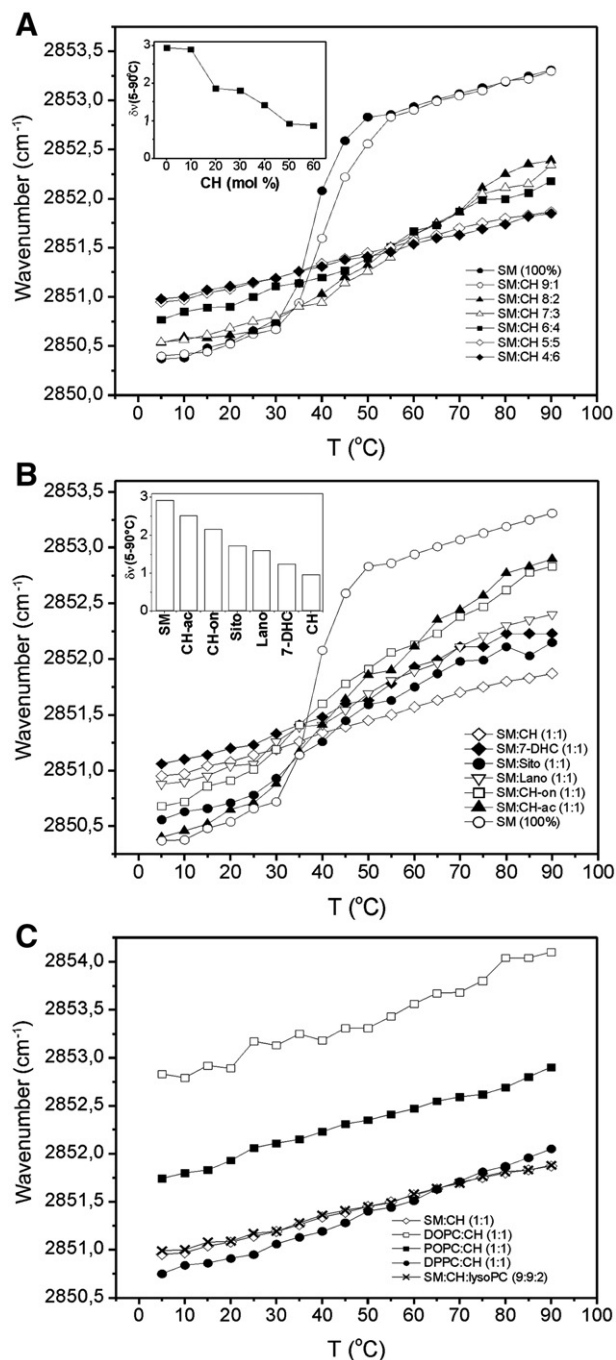
Fig. 2. Wavenumber versus temperature plots of the symmetric CH₂ stretching band of sonicated liposomes composed of (A) sphingomyelin (SM) and cholesterol (CH) in different molar ratios (inset: influence of the SM/CH molar ratio on wavenumber shift ($\delta\nu$) from 5 to 90 °C); (B) different steroids and sphingomyelin in a 1:1 molar ratio (inset: influence of the steroid component on $\delta\nu$ from 5 to 90 °C); and (C) different phospholipids and cholesterol. Each point is the mean value of two independent measurements (standard error was lower than 5%). Other abbreviations are as given in Fig. 1.

5-cholesten-3-one) steroids, all at 1:1 molar ratios (Fig. 2B), were determined. Of all the steroids tested, cholesterol showed the smallest wavenumber shift from 5 to 90 °C (Fig. 2B, inset), and complete absence of a phase transition, suggesting that this sterol induces the complete elimination of the cooperative gel-to-liquid phase transition within the temperature range tested. Of all the other natural sterols with the intact 3-OH group, 7-dehydrocholesterol behaved most similarly to cholesterol, confirming reported results [3,17], and showing that this sterol can induce the formation of an l_o phase. In

liposomes containing other sterols of natural origin (β-sitosterol and lanosterol), a phase transition around 40 °C is still visible. The lower ability of phytosterols (β-sitosterol) to induce the formation of an l_o phase in sterol:PC membranes has already been reported [18], as well as the low phospholipid-condensing potential of lanosterol [19–21]. Liposomes containing steroids with modified – OH groups (5-cholesten-3-one and cholesteryl acetate) displayed the steepest dependence of wavenumber on temperature, which is in accordance with the reduced ability of these steroids to induce the formation of an l_o phase [22–24].

3.1.3. FTIR analysis of equimolar cholesterol:phospholipid sonicated liposomes

Membrane ordering of liposomes composed of cholesterol and phosphatidylcholines with different degrees of saturation (DOPC, POPC, and DPPC) in a 1:1 molar ratio increases with increasing degree of saturation of the phospholipid (Fig. 2C). DPPC and sphingomyelin— the first bearing fully saturated, and the second predominantly (80%) saturated but very long acyl chains—show similar degrees of ordering, which sharply decrease when these phospholipids are replaced by POPC and, further still, by the fully unsaturated DOPC. Further, the wavenumber shift from 5 to 90 °C was nearly the same in all the lipid mixtures (not shown). The plot of wavenumber versus temperature of equimolar sphingomyelin:cholesterol liposomes supplemented with 10% lysoPC was very closely similar to that obtained with sphingo-myelin:cholesterol (1:1) liposomes (Fig. 2C).

3.2. EPR measurements

The influence of lipid composition on the EPR spectra of the spin probe MeFASL(10,3) incorporated in the membrane of sphingomyelin liposomes containing different concentrations of cholesterol (Fig. 3) or different steroids (Fig. 4) was determined from their EPR spectra. The maximal hyperfine splitting, $2A_{max}$, which is related to an average order parameter of membrane lipids, was obtained from the spectra [25]. More detailed information about the membrane nanodomain structure and ordering and about the dynamics within the domains was obtained by computer simulation of the EPR spectra, in combination with the GHOST condensation method [11] (see Section 2.2.3). Representative GHOST diagrams for the spectra measured at 25 °C are presented in Figs. 6, 7 and 8 for the liposomes labelled with MeFASL(10,3), which reflects the characteristics of the membranes close to the surface. The data obtained with MeFASL(2,11), which provides information about the membrane characteristics in the middle of the membrane, are presented in Fig. 6B and Table 1.

As already mentioned in Section 2.2.3, for each EPR spectrum 200 independent HEO simulation runs were applied, taking into account four different motional modes of the spin probe, i.e. four different domain D types. As is resolved from the GHOST diagrams (Figs. 6–8) in most of the samples the solutions are grouped in three, or in some samples four (sphingomyelin with lanosterol, 5-cholesten-3-one, and cholesteryl acetate in Fig. 7, and sphingomyelin:cholesterol:POPC in Fig. 8.) more or less resolved regions where the values for order parameter and polarity correction factor (S and Pa) are located. Each group of solutions describes the motional mode of spin probe in certain types of membrane domains D1 (the most ordered), D2 (intermediate), and D3 or D4 (the least ordered). The values of parameters S and Pa for a certain type of domains D are within the region determined with the borders of the group. Red spots are the average values of parameters in the group which are taken to describe motional mode of spin probe within the domain D type. Colors within the groups describe the values of other two parameters (broadening constant W—green, and correlation time t_c—red) and the number connected with the group denotes the proportion of the domain D type (proportion of the spin probe with the same motional mode). The average values of order parameters S, polarity correction factors
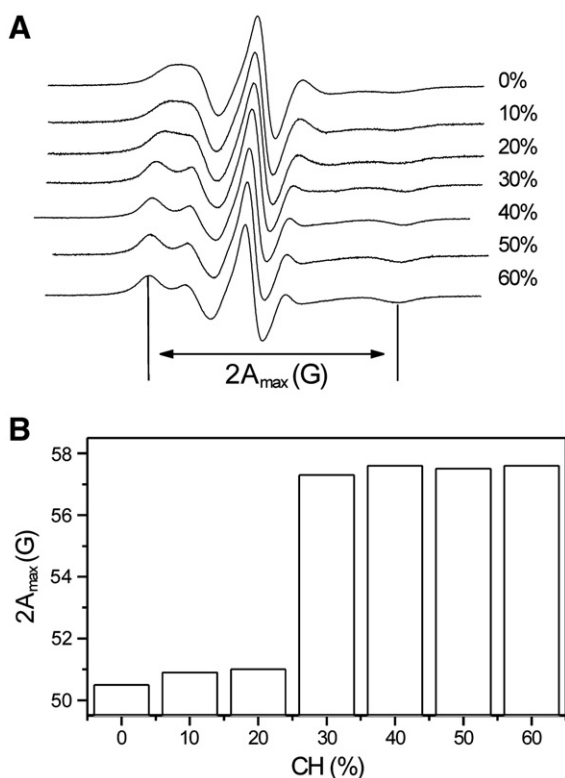
Fig. 3. The influence of the molar ratio of sphingomyelin (SM) to cholesterol (CH) on membrane fluidity characteristics as measured by the MeFASL(10,3) spin probe at 25 °C. A: Representative EPR spectra of MeFASL(10,3) in the membrane of sonicated liposomes composed of sphingomyelin and cholesterol in different molar ratios. Arrow denotes the maximal hyperfine splitting ($2A_{max}$). B: The influence of sphingomyelin: cholesterol molar ratio on $2A_{max}$. Each bar is the mean value of three independent measurements (standard error was lower than 5%).

Fig. 4. The influence of the steroid component of equimolar sphingomyelin (SM): steroid liposomes on membrane fluidity characteristics as measured by MeFASL(10,3) at 25 °C. A: Representative EPR spectra of MeFASL(10,3) in the membrane of sonicated liposomes composed of equimolar sphingomyelin:steroid mixtures. Arrow denotes the maximal hyperfine splitting ($2A_{max}$). B: The influence of steroid component on maximal hyperfine splitting ($2A_{max}$). Each bar is the mean value of three independent measurements (standard error was lower than 5%). Other abbreviations are as given in Fig. 1.

Pa, correlation time t_c, and proportion d for all domain D types are presented in tables below the GHOST diagrams.

In some samples motional patterns in the GHOST diagrams are very close together (e.g. at 0% and 10% cholesterol in Fig. 6, or lanosterol and 5-cholesten-3-one in Fig. 7), indicating that some domain D types are interconnected.

3.2.1. EPR analysis of sphingomyelin:cholesterol sonicated liposomes

At 25 °C, the EPR spectra of cholesterol:sphingomyelin liposomes labelled with MeFASL (10,3) change with increasing mol.% of cholesterol (Fig. 3A). The maximal hyperfine splitting, $2A_{max}$, deduced from experimental spectra, shows an abrupt increase at concentrations ≥30 mol.% cholesterol (Fig. 3B).

In Fig. 5, the temperature dependence of the order parameter (S) and the correlation time (t_c) obtained by computer simulation of the EPR spectra of MeFASL(10,3) in vesicles containing 10 and 50 mol.% cholesterol were compared. Presented are the values of two domain D types that represent the properties of about 95% of the membrane area: one with the highest (D1) and the other with an intermediate value (D2) of order parameter S (Fig. 5). A sudden decrease in the order parameter and increase of t_c at 35 °C was observed for the sample with 10% cholesterol, but not for that with 50 mol.% cholesterol. This agrees well with the data obtained by FTIR (Fig. 2A) and points to a phase transition at this temperature in the liposomes with low concentrations of cholesterol, which disappears at concentrations of more than 30 mol.%.

Analysis of the EPR spectra with the GHOST condensation method (Fig. 6) also shows marked differences in the motional pattern of MeFASL(10,3) between ostreolysin-resistant and ostreolysin-susceptible liposomes, e.g. those containing less than 30 mol.%
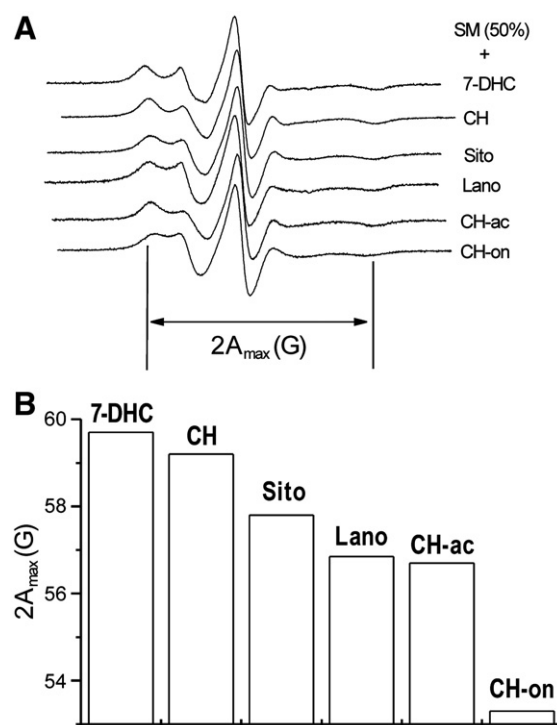
cholesterol, where the liposomes are in the gel phase (s_o) at 25 °C, and more than 30 mol.% cholesterol, where the liposomes are in liquid-ordered (l_o) phase [15] (Fig. 6A). The most pronounced difference is observed in the polarity of the spin probe environment (polarity correction factor, Pa) in the two less ordered domain D types (D3, with the lowest S, and D2, with intermediate S). At concentrations below 30% cholesterol, Pa is close to 1 and increases slightly with increasing proportion of cholesterol in D2. However, in liposomes with more than 30% cholesterol (those exerting the highest susceptibility to ostreolysin), there is a pronounced increase of Pa in the domain D2 type and a concurrent decrease in the domain D3 type. With further increase in cholesterol concentration, the parameters no longer change significantly (Fig. 6A). In contrast to domain D types D2 and D3, the polarity (Pa) and correlation time (t_c) of the spin probe in the most ordered domain D1 type do not change significantly as can be seen comparing the values of parameters presented in tables below GHOST diagrams in Fig. 6A. Only the proportion of D1 increases to some extent. At 20 mol.% cholesterol, it occupies 79% of the whole membrane, while in liposomes containing 30 or more mol.% cholesterol, it occupies ~85–87% of the membrane area. This trend is also accompanied by an increase in the order parameter (Fig. 6A).

In contrast to the results obtained with MeFASL(10,3), GHOST analysis of EPR spectra of liposomes labelled with MeFASL(2,11), which monitors the physical characteristics in the middle of the membrane, shows less pronounced differences in the region between 30 and 40 mol.% cholesterol (Fig. 6B). In sphingomyelin samples without cholesterol only one motional pattern of the spin probe is resolved from the GHOST diagram (results not shown). At 10 and 20 mol.% cholesterol, a domain D type with higher order parameter appeared (D1), and at 30 mol.% another domain D type appeared, that with the lowest order parameter (D3) (Fig. 6B). However, the physical

Table 1
Influence of cholesterol (CH)/sphingomyelin (SM) molar ratio, different phospholipids and steroids on the proportion of membrane domains, order parameter (S), correlation time (t_c) and polarity correction factor (Pa) in sonicated lipid vesicles. Vesicles were labelled with MeFASL(2,11), the spectra taken at 25 °C and analyzed with a GHOST condensation method. D1 represents the most ordered domain, D2 is the domain with intermediate fluidity, and D3 is the most fluid domain. Please refer to the legend Fig.1 for the explanation of other abbreviations used in this table.

Lipid vesicle composition	Proportion (d)			Order parameter (S)			Correlation time t_c (ns)			Polarity correction Pa		
	D1	D2	D3	D1	D2	D3	D1	D2	D3	D1	D2	D3
SM (100%)		1	–	–	0.29	–	–	1.07	–	–	0.976	–
SM:CH (9:1)	0.39	0.61	–	0.61	0.30	–	0.26	0.92	–	1.02	0.97	–
SM:CH (8:2)	0.40	0.60	–	0.49	0.33	–	0.34	0.95	–	1.01	0.93	–
SM:CH (7:3)	0.32	0.39	0.29	0.55	0.36	0.19	0.67	0.47	2.02	1.03	0.93	0.94
SM:CH (6:4)	0.33	0.47	0.20	0.58	0.41	0.21	0.51	0.42	2.75	1.02	0.92	0.93
SM:CH (5:5)	0.31	0.43	0.26	0.60	0.39	0.20	0.52	0.40	2.61	1.03	0.92	0.92
SM:CH (4:6)	0.30	0.43	0.27	0.61	0.38	0.19	0.47	0.38	2.87	1.04	0.92	0.92
CH:DPPC	0.09	0.58	0.33	0.60	0.40	0.24	0.30	0.34	2.04	1.02	0.93	0.91
CH:POPC	–	0.52	0.48	–	0.35	0.18	–	0.31	1.28	–	0.92	0.92
CH:DOPC	–	0.38	0.62	–	0.32	0.14	–	0.37	1.32	–	0.93	0.93
SM:CH:POPC (2:2:1)	0.12	0.41	0.47	0.64	0.35	0.19	0.35	0.39	1.70	1.03	0.93	0.93
SM:CH:lysoPC (9:9:2)	0.33	0.40	0.27	0.60	0.39	0.21	0.40	0.42	2.64	1.03	0.93	0.92
SM:7-DHC	0.16	0.55	0.29	0.65	0.38	0.19	0.46	0.35	2.40	1.06	0.92	0.92
SM:Sito	0.37	0.30	0.33	0.54	0.37	0.14	0.28	0.59	1.82	1.02	0.94	0.96
SM:Lano	0.75	0.22	0.03	0.41	0.19	0.16	0.37	2.44	0.49	0.93	0.93	0.81
SM:CH-on	0.22	0.40	0.38	0.58	0.36	0.17	0.30	0.35	2.07	1.03	0.94	0.91
SM:CH-ac	0.40	0.38	0.22	0.59	0.39	0.19	0.38	0.72	2.61	1.02	0.93	0.95

characteristics of these domains are much less influenced by cholesterol than in the upper part of the membrane as detected with MeFASL(10,3).

3.2.2. EPR analysis of equimolar sphingomyielin:steroid sonicated liposomes

The maximal hyperfine splitting, deduced from EPR spectra of sphingomyelin:steroid liposomes labelled with MeFASL(10,3) at 25 °C, is consistent with reported data on the ordering characteristics

Fig. 5. Temperature dependence of order parameter, S, (A) and correlation time, t_c, (B) of MeFASL(10,3) in the membranes of sphingomyelin (SM):cholesterol (CH) liposomes at respectively 5:5 and 9:1 mol.%. S and t_c were calculated from the line shape of the EPR spectra by the HEO simulation procedure with GHOST condensation routine [11]. The parameters of the most ordered (D1) and intermediately ordered domain D2 types are presented. Each point corresponds to the mean value of three independent measurements (standard error was lower than 5%).

of different steroids [17–24]. 7-dehydrocholesterol readily induces the ordering of surrounding phospholipids, while the liposomes containing lanosterol or synthetic steroids with low ordering ability show lower $2A_{max}$ values (Fig. 4).

According to GHOST analysis, MeFASL(10,3) in ostreolysin-susceptible sphingomyelin liposomes supplemented with 7-dehydrocholesterol and β-sitosterol experiences a similar motional pattern to that in sphingomyelin:cholesterol liposomes with more than 30 mol.% cholesterol (Fig. 7). The results indicate three well-resolved domain D types with characteristic differences in polarity; Pa is high in D2 and very low in D3. The most ordered domain D1 type, with order parameter $S > 0.72$, occupies 80% or more of the membrane area ($d ≥ 0.8$), and is clearly separated from the less ordered domain D2 and D3 types. The motional patterns of MeFASL(10,3) in ostreolysin-resistant liposomes containing other sterols or cholesterol derivatives (lanosterol, 5-cholesten-3-one and cholesteryl acetate) differ markedly from the above-mentioned patterns and also, considerably, from each other (Fig. 7).

Comparison of the calculated parameters (tables below GHOST diagrams in Fig. 7) with the values of $2A_{max}$ measured directly from the spectra (Fig. 4) shows that the value of $2A_{max}$ reflects the order parameter of the most ordered domain D1 type, which occupies the highest proportion of the membrane in all the measured liposomes ($d > 66\%$). Liposomes containing 7-dehydrocholesterol and cholesterol (the corresponding order parameters of the most ordered domain D1 type are $S = 0.77$ and 0.75, respectively) exhibit the largest values of $2A_{max}$. In other samples, order parameter S in the most ordered domain D1 type was less than 0.76 or the proportion of D1 was less than 80%. Again, the properties of the most highly ordered domain D1 type do not change much between different steroids, irrespective of their influence on ostreolysin membrane activity, indicating that the properties of the less ordered domain D types in the upper part of the membrane are important for ostreolysin binding.

No correlation between the GHOST pattern and membrane binding and pore-forming activity of ostreolysin was observed using MeFASL(2,11) (Fig. 1, Table 1), indicating that the changes in the domain structure caused by steroids in the middle of the membrane are not a prerequisite for the activity of the protein.

3.2.3. EPR analysis of phospholipid:cholesterol sonicated liposomes

Phospholipids with different degrees of saturation influence ostreolysin binding (Fig. 1), membrane fluidity (Fig. 2), and motional pattern of MeFASL(10,3) (Fig. 8). The GHOST diagrams (Fig. 8) show
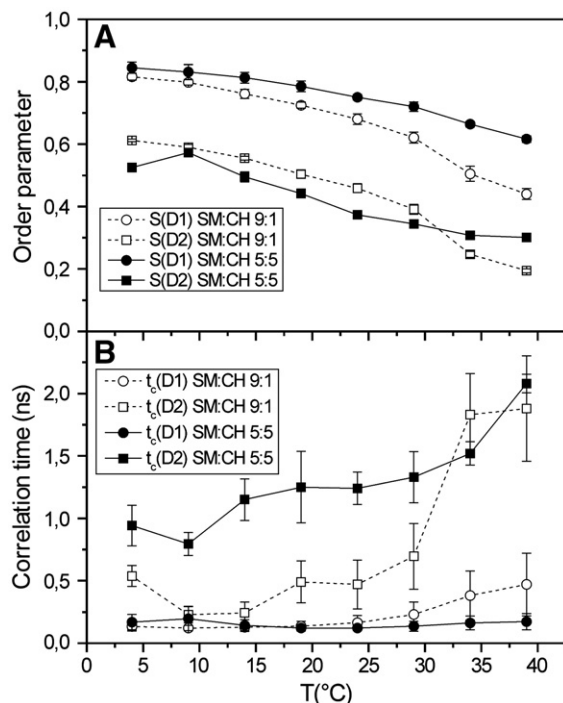
A

MeFASL(10,3)

0% CH

Pa (1) vs S (1)

D2 D1
13 87

domain	d	S	tc (ns)	Pa
D1	0.87	0.6	0.25	1.01
D2	0.13	0.26	2.56	1

10% CH

Pa (1) vs S (1)

D3 D2 D1
6 21 74

domain	d	S	tc (ns)	Pa
D1	0.74	0.68	0.16	1.01
D2	0.2	0.46	0.46	1
D3	0.06	0.24	1.27	1

20% CH

Pa (1) vs S (1)

D2 D1
16 79
D3
5

domain	d	S	tc (ns)	Pa
D1	0.79	0.71	0.14	1
D2	0.16	0.45	0.64	1.01
D3	0.05	0.1	2.72	0.94

30% CH

Pa (1) vs S (1)

11
D2
D3 D1
85
4

domain	d	S	tc (ns)	Pa
D1	0.85	0.74	0.15	1.01
D2	0.11	0.48	0.97	1.07
D3	0.04	0.09	2.51	0.98

40% CH

Pa (1) vs S (1)

10
D2
D1
87
D3
3

domain	d	S	tc (ns)	Pa
D1	0.87	0.75	0.13	1.02
D2	0.11	0.38	1.48	1.17
D3	0.03	0.25	0.79	0.85

50% CH

Pa (1) vs S (1)

11
D2
D1
86
D3
3

domain	d	S(1)	tc(ns)	Pa(1)
D1	0.86	0.75	0.12	1.01
D2	0.11	0.37	1.25	1.17
D3	0.03	0.23	0.99	0.84

60% CH

Pa (1) vs S (1)

12
D2
D1
85
D3
3

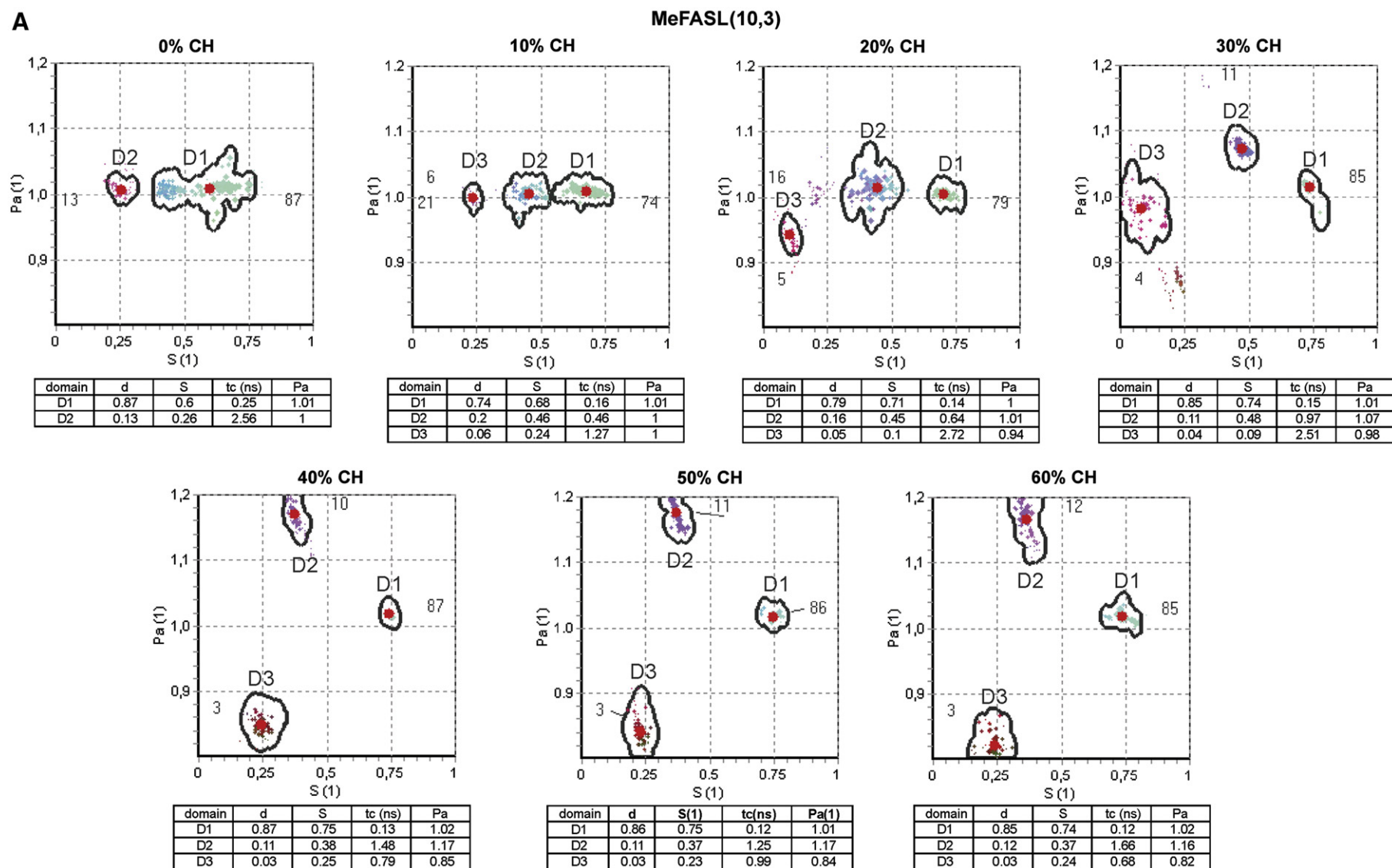| domain	d	S	tc (ns)	Pa
D1	0.85	0.74	0.12	1.02
D2	0.12	0.37	1.66	1.16
D3	0.03	0.24	0.68	0.82

Fig. 6. S— Pa (order parameter–polarity correction factor) GHOST diagrams that define the motional modes of MeFASL(10,3) (A) or MeFASL (2,11) (B) spin probe at 25 °C in the membrane of sonicated liposomes composed of sphingomyelin and cholesterol (CH) in different molar ratios, and give information about the membrane domain D types. The numbers in the tables below each GHOST diagram are the average values of spectral parameters (red dots) obtained from multiple runs of the HEO optimization procedure, which give the best fits to the experimental spectra. Borders of each group determine the interval where the solutions can be obtained. D1, D2 and D3 denote the most, intermediate and least ordered domain D types, d = proportion of the domain, S = order parameter, t_c = rotational correlation time, Pa = polarity correction factor of the hyperfine splitting tensor.
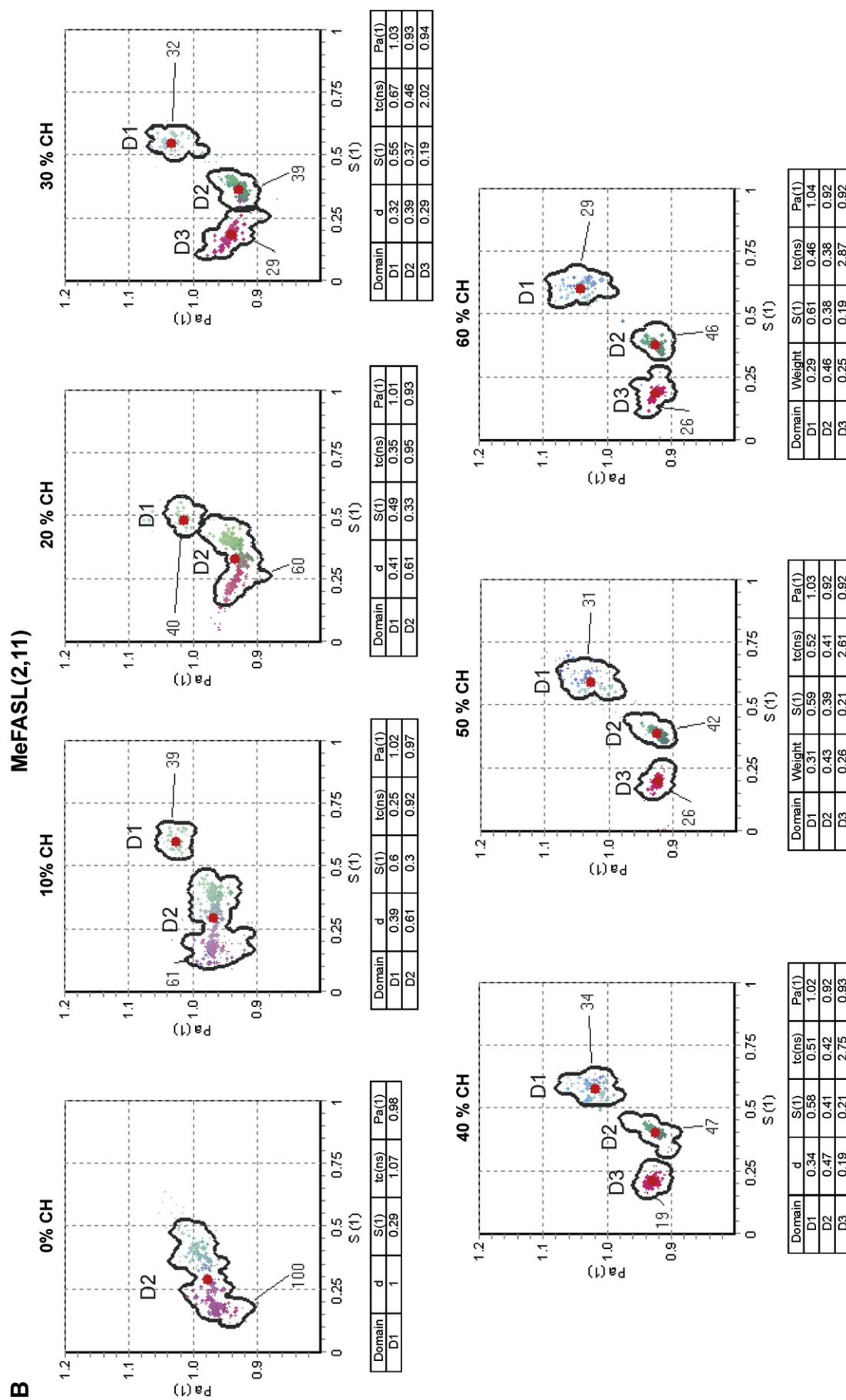
Fig. 6 (*continued*).

SM:CH (1:1)

domain	d	S(1)	tc(ns)	Pa(1)
D1	0.86	0.75	0.12	1.01
D2	0.11	0.37	1.25	1.17
D3	0.03	0.23	0.99	0.84

SM:7-DHC (1:1)

domain	d	S(1)	tc(ns)	Pa(1)
D1	0.84	0.77	0.15	1.02
D2	0.1	0.52	0.93	1.09
D3	0.06	0.12	1.95	0.96

SM:Sito (1:1)

domain	d	S(1)	tc(ns)	Pa(1)
D1	0.8	0.72	0.12	1.02
D2	0.16	0.41	2.24	1.1
D3	0.04	0.17	1.68	0.87

SM:Lano (1:1)

domain	d	S(1)	tc(ns)	Pa(1)
D1	0.66	0.75	0.14	1
D2	0.22	0.63	0.15	1.01
D3	0.04	0.52	0.46	1.04
D4	0.08	0.13	2.96	0.9

SM:CH-on (1:1)

domain	d	S(1)	tc(ns)	Pa(1)
D1	0.74	0.71	0.17	1
D2	0.04	0.5	0.59	1
D3	0.16	0.38	2.42	1.01
D4	0.06	0.16	1.86	0.88

SM:CH-ac (1:1)

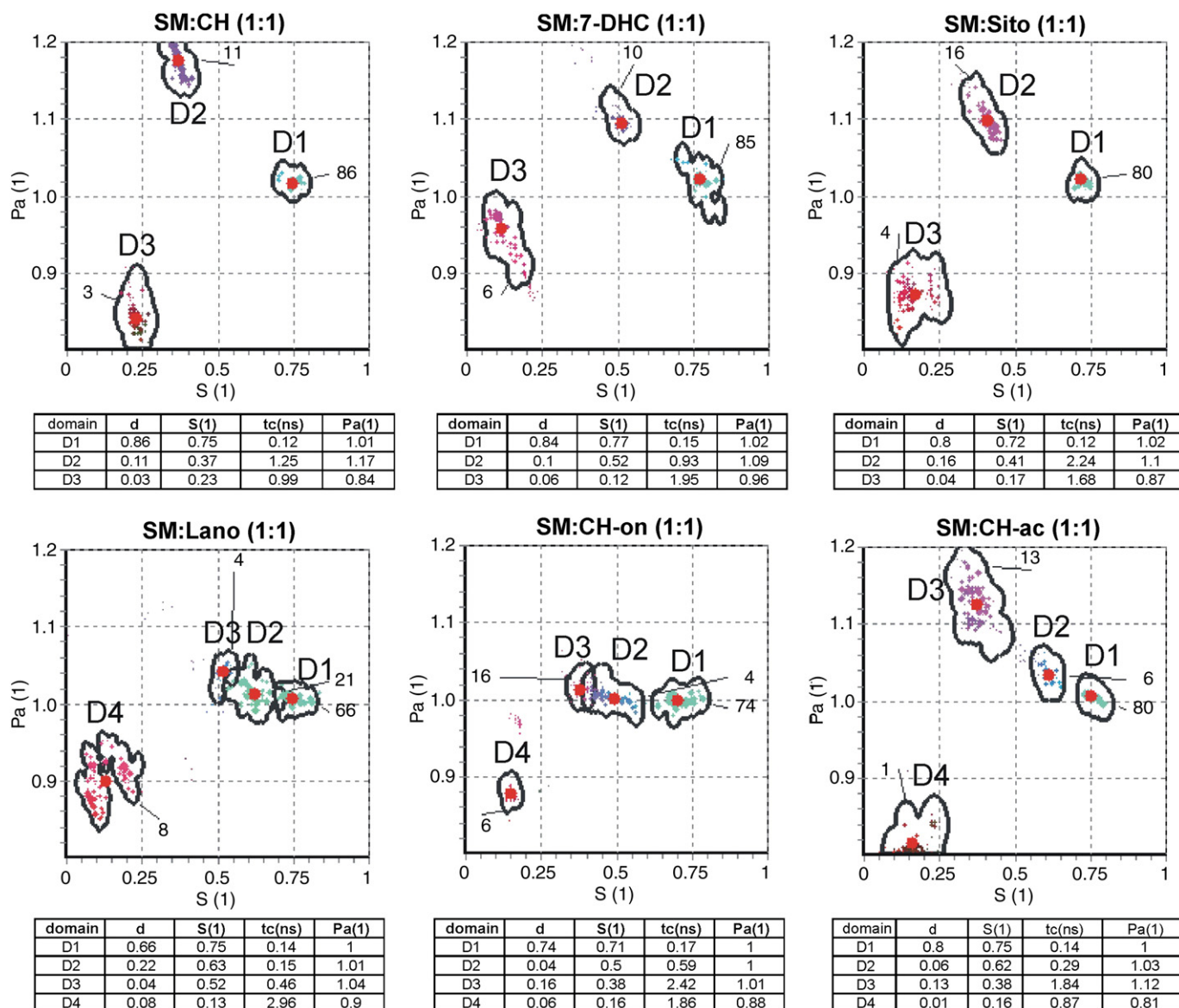| domain	d	S(1)	tc(ns)	Pa(1)
D1	0.8	0.75	0.14	1
D2	0.06	0.62	0.29	1.03
D3	0.13	0.38	1.84	1.12
D4	0.01	0.16	0.87	0.81

Fig. 7. S–Pa GHOST diagrams defining motional modes of MeFASL(10,3) spin probe in the membranes of sonicated liposomes composed of sphingomyelin (SM) and different steroids in a 1:1 molar ratio at 25 °C. D1, D2, D3 and D4 denote the most, intermediate and least ordered domain D types, d = proportion of the domain, S = order parameter, t_c = rotational correlation time, Pa = polarity correction factor of the hyperfine splitting tensor. Steroid abbreviations as in Fig 1.

that even small amounts of mono-unsaturated POPC significantly change the motional pattern of the spin probe. The typical motional pattern, with well-resolved domain D types and large differences in Pa, characteristic for the liposomes which bind ostreolysin, is lost. Similar motional pattern as with POPC is obtained also with DOPC. With increasing amount of DOPC proportion of the most ordered domain D1 type decreases, but also the order parameter and polarity of all domain D types decrease, indicating that lipids with unsaturated acyl chains contribute to all the domains (results not shown). The polarity of the intermediate domain D2 type decreases, together with the order parameter and proportion of the most ordered domain D1 type. The same behaviour is observed for liposomes in which sphingomyelin is completely replaced by POPC or DOPC. In liposomes where sphingomyelin is replaced by DPPC, the typical motional pattern is still preserved, but the order parameter of the most ordered domain decreases.

The GHOST diagram of sphingomyelin:cholesterol liposomes supplemented with 10% lysoPC did not differ significantly from that obtained with equimolar sphingomyelin:cholesterol liposomes, and

the calculated parameter remains within the range of experimental error (Fig. 8).

4. Discussion

Due to its specific interaction with sterol/sphingolipid-enriched membrane regions, ostreolysin and, particularly, its labelled non-toxic mutants could be good candidates as molecular markers for raft-like membrane domains [5]. For this reason, here we have further investigated how characteristics of nanoscale domains, investigated by FTIR and EPR, of artificial membranes susceptible to ostreolysin, correlate with its membrane binding and pore-forming activity. In sphingomyelin:cholesterol liposomes, both binding and permeabilization take place above 30 mol.% membrane cholesterol [2,3] (Fig. 1A and B). At lytic concentrations used in our experiments ostreolysin itself does not perturb membrane fluidity as revealed by EPR before [2]. Possible changes of phospholipid ordering and dynamics in the vicinity of pores formed by ostreolysin thus seem to be not extensive enough to be resolved by EPR using MeFASL as spin probes. Its
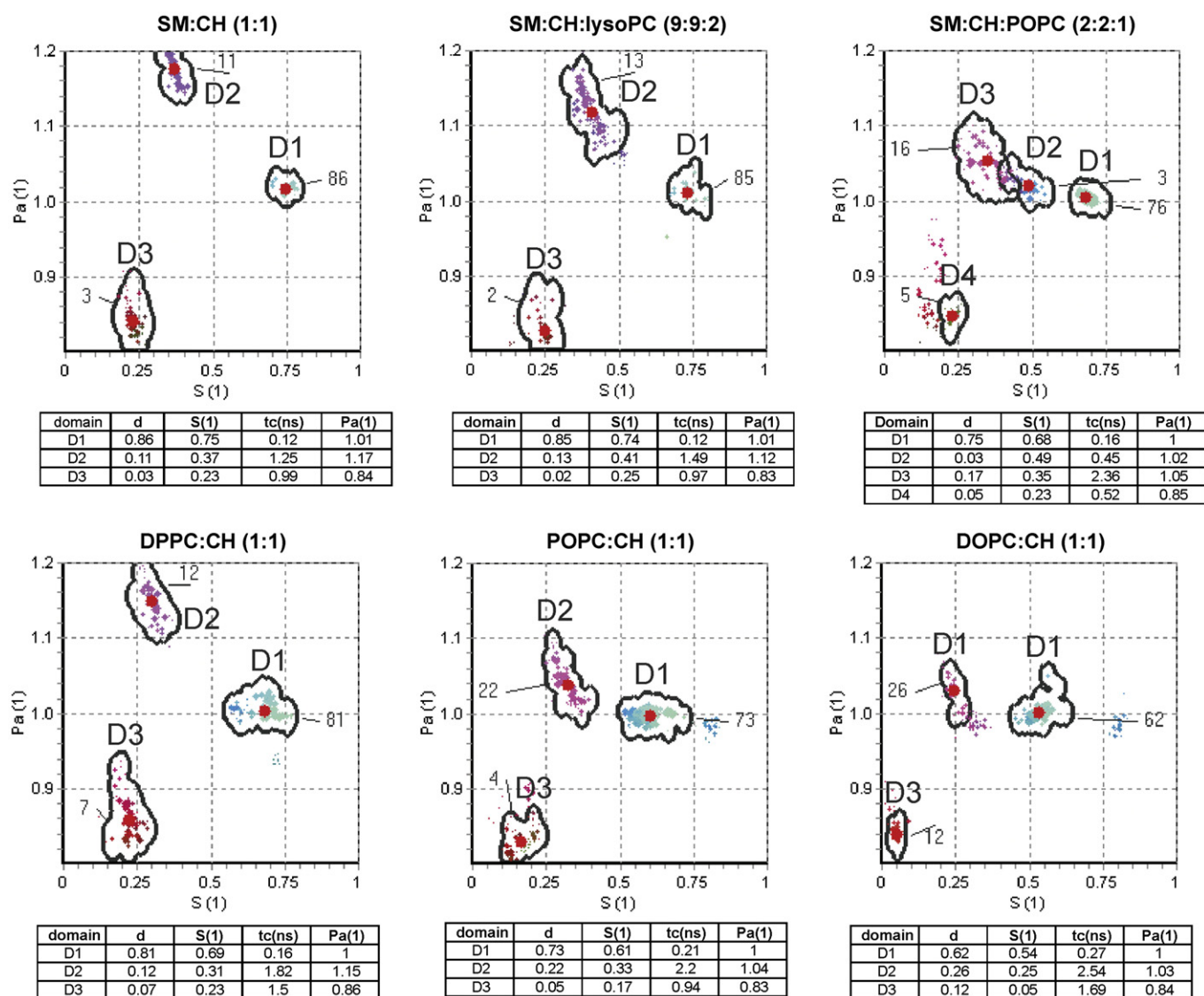
SM:CH (1:1)

domain	d	S(1)	tc(ns)	Pa(1)
D1	0.86	0.75	0.12	1.01
D2	0.11	0.37	1.25	1.17
D3	0.03	0.23	0.99	0.84

SM:CH:lysoPC (9:9:2)

domain	d	S(1)	tc(ns)	Pa(1)
D1	0.85	0.74	0.12	1.01
D2	0.13	0.41	1.49	1.12
D3	0.02	0.25	0.97	0.83

SM:CH:POPC (2:2:1)

Domain	d	S(1)	tc(ns)	Pa(1)
D1	0.75	0.68	0.16	1
D2	0.03	0.49	0.45	1.02
D3	0.17	0.35	2.36	1.05
D4	0.05	0.23	0.52	0.85

DPPC:CH (1:1)

domain	d	S(1)	tc(ns)	Pa(1)
D1	0.81	0.69	0.16	1
D2	0.12	0.31	1.82	1.15
D3	0.07	0.23	1.5	0.86

POPC:CH (1:1)

domain	d	S(1)	tc(ns)	Pa(1)
D1	0.73	0.61	0.21	1
D2	0.22	0.33	2.2	1.04
D3	0.05	0.17	0.94	0.83

DOPC:CH (1:1)

domain	d	S(1)	tc(ns)	Pa(1)
D1	0.62	0.54	0.27	1
D2	0.26	0.25	2.54	1.03
D3	0.12	0.05	1.69	0.84

Fig. 8. S–Pa GHOST diagrams defining motional modes of MeFASL(10,3) spin probe at 25 °C in the membranes of sonicated liposomes composed of equimolar mixtures of cholesterol (CH) and other phospholipids (sphingomyelin (SM), dipalmitoylphosphatidylcholine (DPPC), palmitoyl-oleoylphosphatidylcholine (POPC), and dioleoylphosphatidylcholine (DOPC)), equimolar mixtures of SM and CH with the addition of 10% palmitoyl-lysophosphatidylcholine (lysoPC) or 20% POPC. D1, D2, D3 and D4 denote the most, intermediate and least ordered domain types, d = proportion of the domain, S = order parameter, t_c = rotational correlation time, Pa = polarity correction factor of the hyperfine splitting tensor.

membrane activity in equimolar cholesterol:phospholipid liposomes decreases sharply on replacing sphingomyelin by other glycerophospholipids, in particular those bearing unsaturated acyl chains, or on introducing low concentrations of lysophospholipids [2,5] (Fig. 1C and D). In sphingomyelin liposomes supplemented with different sterols or synthetic cholesterol derivatives, ostreolysin membrane activity decreases on modifying the sterol 3β-OH group, or by introducing additional double bonds or methylation of the steroid skeleton or C17-isooctyl chain. Liposomes displaying the highest susceptibility to ostreolysin are those containing cholesterol, β-sitosterol and 7-dehydrocholesterol [3] (Fig. 1E and F).

The ability of ostreolysin to bind and permeabilize sphingomyelin: cholesterol membranes only above 30 mol.% of membrane cholesterol, its association with detergent-resistant membranes of both cells and artificial lipid vesicles, and the impairment of its membrane activity by membrane treatment with the cholesterol scavenger methyl-β-cyclodextrin, all point to the specific interaction of this protein with sterol/sphingomyelin-enriched membranes existing in the l_o phase or with cell membrane lipid rafts [2,3,5]. The exact mechanism of ostreolysin membrane action is not yet fully understood due to the

lack of information on ostreolysin tertiary structure. The protein sequence however contains two cysteine, and six tryptophan residues [26], and this combination has been proposed to be involved in sterol binding of cholesterol-dependent bacterial pore-forming toxins [27]. Furthermore, the experiments with liposomes composed of equimolar sphingomyelin:steroid mixtures clearly showed that ostreolysin membrane activity does not correlate completely with the ability of a given steroid to promote the formation of the l_o phase [3]. This activity is always highest with cholesterol-containing membranes, although their order parameter is not the highest. Also, it is high in liposomes containing β-sitosterol, although this sterol displays low ordering ability [18] (Fig. 1E and F). Finally, increasing the proportion of cholesterol in cholesterol:sphingomyelin liposomes enhances ostreolysin binding in a highly cooperative manner, suggesting that the lateral distribution and accessibility of the sterols at the membrane surface are crucial for its activity [3].

To further elucidate the membrane structural determinants that lead to ostreolysin binding, we have studied the ordering of membrane lipids using FTIR and EPR. In general, both methods show significant increase in membrane ordering at cholesterol

concentrations higher than 30 mol.%, and some indication that cholesterol, 7-dehydrocholesterol and sitosterol have higher ordering than the other investigated sterols. There are some differences between the results obtained with the two methods, which is not surprising as the approaches used are very different. By FTIR, the frequency of vibration of fatty acid methylene groups is measured, while EPR monitors motional characteristics of the spin probe which has to be introduced into the membrane and reflects ordering and dynamics of its surrounding. However, the methods are comparable and complementary as by EPR the membrane heterogeneity and membrane domain characteristics on the nm scale could be determined by computer analysis of EPR spectra. Most of the data were analyzed at 25 °C, the temperature at which most of previous membrane binding and permeabilization studies of ostreolysin were performed [2–4].

In sphingomyelin:cholesterol membranes at 25 °C, the membrane binding and pore-forming activity of ostreolysin correlate with the formation of an l_o phase, both phenomena occurring above 30% of cholesterol [2,3,15] (Fig. 1A and B). The formation of the l_o phase at these lipid compositions, indicated by reduction of the wavenumber shift between 5 and 90 °C, and by the disappearance of phase transitions, was confirmed by FTIR analysis and EPR (Figs. 2A and 5). It derives from the ability of cholesterol to condense the surrounding sphingomyelin molecules [13], thus increasing the lipid ordering in the membrane.

It is worthy to recall that EPR spectroscopy gives information on membrane properties at a molecular level. It measures local (segmental) conformational entropy but not the free enthalpy of the molecule as a whole, not even the entropy of a molecule. The latter is combined from entropy due to lateral diffusion as well as due to rotational diffusion of all the tail segments and not only the one segment which is measured by EPR. This means that the motional patterns (local ordering) can be more or less heterogeneous than it can be deduced from free enthalpy measurements. Therefore definition of a "phase" originating from calorimetric free enthalpy change measurements is not necessarily applied at the molecular level. Computer simulation of EPR spectra showed that cholesterol induces remarkable changes in the motional pattern of MeFASL(10,3), which reflects characteristics of lateral membrane domain D types on the nm scale close to the membrane surface (Fig. 6A). Typically, the spin probe experiences three types of motional modes, those are interconnected at low cholesterol but separate at higher cholesterol concentrations. Above 30 mol.% cholesterol, i.e. in the l_o phase, there is an abrupt change in the characteristics of the less ordered domain D types (D2 and D3), which is reflected in all parameters measured (Tables in Fig. 6A), but is optimally observed in the polarity of the spin probe surrounding (Fig. 6A). These data indicate that, in the l_o phase and in some parts of the membrane, the spin probes become more accessible to polar molecules (probably water and sterol hydroxyls), while a small proportion of the spin probes (less than 5%) appear to be driven deeper into the membrane bilayer or into regions with a lower concentration of water and sterol hydroxyls as Pa decreases to 0.85. For the most ordered domain D1 type, the order parameter increases to $S = 0.75$ and its proportion from 79 to 85%. Only the changes in the upper part of the membrane appear to be responsible for ostreolysin binding, the properties in the middle of the membrane being less important.

As to the liposomes composed of equimolar mixtures of sphingomyelin and different steroids, the results of FTIR measurements (Fig. 2B) are compatible with those in our previous study [3], in which differential scanning calorimetry (DSC) and steady-state 1,6-diphenyl-1,3,5-hexatriene (DPH) anisotropy were used to characterize the phase state of some of the equimolar sphingomyelin:steroid liposomes. DSC thermograms, recorded in the temperature range from 0 to 70 °C, were significantly broadened, pointing to the existence of several lipid phases, as expected for the high content of steroids. The

combined results obtained in this and the previous study [3] confirm that the steroid structure promoting the formation of the most ordered domains is not critical for ostreolysin membrane binding and pore-forming activity. Similar findings were recently reported for another cholesterol-binding cytolysin, perfringolysin O [28]. Further, maximal hyperfine splitting, which is a measure of the average order parameter (Fig. 4), and GHOST diagrams of EPR-spectral components (Fig. 7) reveal that sterols and cholesterol derivatives have different abilities to induce changes in membrane domain characteristics. Again, the ability of ostreolysin to exert its membrane activity is not directly correlated with the ordering potential of steroids. For example, the ordering potential is highest for sphingomyelin liposomes containing 7-dehydrocholesterol (Figs. 4 and 7) that, in contrast, exert lower susceptibility to ostreolysin binding than the liposomes supplemented with cholesterol or β-sitosterol (Fig. 1E and F). On the other hand, ostreolysin binding correlates with the particular motional pattern of MeFASL(10,3) in GHOST diagrams (Fig. 7), which is nearly identical to that observed in sphingomyelin:cholesterol liposomes with >30% membrane cholesterol, and is similarly not influenced by the changes in the membrane interior.

Indeed, all the liposomes that are susceptible to ostreolysin (sphingomyelin:cholesterol liposomes with ≥40 mol.% cholesterol, and equimolar sphingomyelin/7-dehydrocholesterol or β-sitosterol liposomes, see Fig. 1) appear to share similar GHOST patterns, in which the most ordered domain D1 type exceeds 80% of the whole membrane and is clearly resolved from the other two domain D types that differ characteristically in the polarity correction factor Pa (high Pa in D2 and very low Pa in D3). A similar motional pattern is also observed for the equimolar cholesterol:DPPC liposomes that are less susceptible to ostreolysin, which also form l_o phase but with an order parameter of the most ordered domain D type that is lower than that of equimolar sphingomyelin:cholesterol liposomes (Fig. 8). This result suggests that the l_o phase is not homogeneous, but consists of several regions with different physical characteristics characterised by a specific motional pattern that may exist on the nanometre scale. However, for effective ostreolysin binding it appears that the proportion of the most ordered domain D type should comprise at least 80% of the membrane, and that its order parameters should be more than 0.72.

Further, the fluidity and the membrane domain characteristics of sphingomyelin:cholesterol liposomes containing 10% lysoPC did not differ from those lacking the lysophospholipid (Figs. 2C and 8). The latter are obviously not implied in changing the membrane ordering or domain rearrangement of sphingomyelin:cholesterol membranes, so the mechanism of its strong inhibition of ostreolysin membrane activity [4,5] remains to be established.

5. Conclusions

Our results suggest that, for full membrane binding and pore-forming activity, ostreolysin requires a high degree of membrane ordering accompanied by a specific lateral distribution of cholesterol and sphingomyelin (or saturated phosphatidylcholine) molecules in the plane of the membrane at nm scale. The results obtained from GHOST analysis of the EPR spectra (Figs. 6–8) reveal that, regardless of their lipid compositions, ostreolysin-susceptible membranes exhibit a similar motional pattern of the MeFASL(10,3) spin probe, with a characteristic difference in the polarity factor (Pa) of domain D2 and D3 types. In all these membranes, the order parameter of the most ordered domain D1 type is greater than 0.72, and covers 80% or more of the membrane area. How these domains of D type are distributed in the membrane with respect to others, and what the size of the domains is, remains to be elucidated. Recently, there have been several reports on structural microheterogeneity of coexisting raft-like membrane assemblies at nanometre scale [5,29–34]. These findings, combined with the fact that ostreolysin recognizes cholesterol-enriched

membrane microdomains that are different from those binding caveolin or cholera toxin B subunit [5], suggest that these membrane lateral microheterogeneities could have a crucial role in the binding of, and permeabilization induced by ostreolysin.

In agreement with its pore-forming mechanism ([4] and manuscript in revision), lytic concentrations of ostreolysin do not induce a detectable change in the EPR spectra of equimolar sphingomyelin: cholesterol mixtures [2], indicating that the protein does not induce significant fluidity changes in the membrane on binding and permeabilization. Similarly, FTIR studies revealed that the protein does not modify the fluidity of the membrane of liposomes prepared from sheep erythrocyte lipids [4]. It is thus tempting to speculate that the membrane binding of ostreolysin derives from its recognition of a specific binding site on cholesterol/sphingomyelin assemblies or their boundaries to other nanodomains, all distributed in the membrane plane. It is known that such transient nanostructures, formed by hydrogen bonding [35] and/or according to the "umbrella" model, are typical for cholesterol/sphingomyelin-rich membranes and lipid rafts [6]. Interestingly, in contrast to ostreolysin, a cholesterol-dependent cytolysin, perfringolysin, requires more exposed and free cholesterol molecules such as found in more fluid membranes containing unsaturated phospholipids [36].

Acknowledgements

References

[1] S. Berne, I. Križaj, F. Pohleven, T. Turk, P. Maček, K. Sepčić, *Pleurotus* and *Agrocybe* hemolysins, new proteins hypothetically involved in fungal fruiting, Biochim. Biophys. Acta 1570 (2002) 153–159.
[2] K. Sepčić, S. Berne, K. Rebolj, U. Batista, A. Plemenitaš, M. Šentjurc, P. Maček, Ostreolysin, a pore-forming protein from the oyster mushroom, interacts specifically with membrane cholesterol-rich lipid domains, FEBS Lett. 575 (2004) 81–85.
[3] K. Rebolj, N. Poklar Ulrih, P. Maček, K. Sepčić, Steroid structural requirements for interaction of ostreolysin, a lipid-raft binding cytolysin, with lipid monolayers and bilayers, Biochim. Biophys. Acta 1758 (2006) 1662–1670.
[4] K. Sepčić, S. Berne, C. Potrich, T. Turk, P. Maček, G. Menestrina, Interaction of ostreolysin, a cytolytic protein from the edible mushroom *Pleurotus ostreatus*, with lipid membranes and modulation by lysophospholipids, Eur. J. Biochem. 270 (2003) 1199–1210.
[5] H.H. Chowdhury, K. Rebolj, M. Kreft, R. Zorec, P. Maček, K. Sepčić, Lysophospholipids prevent binding of a cytolytic protein ostreolysin to cholesterol-enriched membrane domains, Toxicon 51 (2008) 1345–1356.
[6] D. Lingwood, K. Simons, Lipid rafts as a membrane-organizing principle, Science 327 (2010) 46–50.
[7] E. Maličev, H.H. Chowdhury, P. Maček, K. Sepčić, Effect of ostreolysin, an Asp-hemolysin isoform, on human chondrocytes and osteoblasts, and possible role of Asp-hemolysin in pathogenesis, Med. Mycol. 45 (2007) 123–130.
[8] J.H. Crowe, F. Tablin, N. Tsvetkova, A.E. Oliver, N. Walker, L.M. Crowe, Are lipid phase transitions responsible for chilling damage in human platelets? Cryobiology 38 (1999) 180–191.
[9] J. Štrancar, M. Šentjurc, M. Schara, Fast and accurate characterization of biological membranes by EPR spectral simulations of nitroxides, J. Magn. Reson. 142 (2000) 254–265.
[10] J. Štrancar, T. Koklič, Z. Arsov, Soft picture of lateral heterogeneity in biomembranes, J. Membr. Biol. 196 (2003) 135–146.
[11] J. Štrancar, T. Koklič, Z. Arsov, B. Filipič, D. Stopar, M.A. Hemminga, Spin label EPR-based characterization of biosystem complexity, J. Chem. Inf. Comput. Sci. 45 (2005) 394–406.

[12] K. Vrhovnik, J. Kristl, M. Šentjurc, J. Šmid-Korbar, Influence of liposome bilayer fluidity on the transport of encapsulated substance into the skin as evaluated by EPR, Pharm. Res. 15 (1998) 523–529.
[13] W.C. Hung, M.T. Lee, F.Y. Chen, H.W. Huang, The condensing effect of cholesterol in lipid bilayers, Biophys. J. 92 (2007) 3960–3967.
[14] J. Aittoniemi, P.S. Niemelä, M.T. Hyvönen, M. Karttunen, I. Vattulainen, Insight into the putative specific interactions between cholesterol, sphingomyelin, and palmitoyl-oleoyl phosphatidylcholine, Biophys. J. 92 (2007) 1125–1137.
[15] R.F. de Almeida, A. Fedorov, M. Prieto, Sphingomyelin/phosphatidylcholine/cholesterol phase diagram: boundaries and composition of lipid rafts, Biophys. J. 85 (2003) 2406–2416.
[16] Z. Arsov, L. Quaroni, Detection of lipid phase coexistence and lipid interactions in sphingomyelin/cholesterol membranes by ATR-FTIR spectroscopy, Biochim. Biophys. Acta 1778 (2008) 880–889.
[17] X. Xu, R. Bittman, G. Duportail, D. Heissler, C. Vilcheze, E. London, Effect of the structure of natural sterols and sphingolipids on the formation of ordered sphingolipid/sterol domains (rafts). Comparison of cholesterol to plant, fungal, and disease-associated sterols and comparison of sphingomyelin, cerebrosides, and ceramide, J. Biol. Chem. 276 (2001) 33540–33546.
[18] K.K. Halling, J.P. Slotte, Membrane properties of plant sterols in phospholipid bilayers as determined by differential scanning calorimetry, resonance energy transfer and detergent-induced solubilization, Biochim. Biophys. Acta 1664 (2004) 161–171.
[19] X. Xu, E. London, Effect of the structure of natural sterols and sphingolipids on the formation of ordered sphingolipid/sterol domains (rafts). Comparison of cholesterol to plant, fungal, and disease-associated sterols and comparison of sphingomyelin, cerebrosides, and ceramide, Biochemistry 39 (2000) 844–849.
[20] P.L. Yeagle, R.B. Martin, A.K. Lala, H.K. Lin, K. Bloch, Differential effects of cholesterol and lanosterol on artificial membranes, Proc. Natl. Acad. Sci. U.S.A. 74 (1977) 4924–4926.
[21] J.A. Urbina, S. Pekerar, H.B. Le, J. Patterson, B. Montez, E. Oldfield, Molecular order and dynamics of phosphatidylcholine bilayer membranes in the presence of cholesterol, ergosterol and lanosterol: a comparative study using 2H-, 13C- and 31P-NMR spectroscopy, Biochim. Biophys. Acta 1238 (1995) 163–176.
[22] V. Ben-Yashar, Y. Barenholz, The interaction of cholesterol and cholest-4-en-3-one with dipalmitoylphosphatidylcholine. Comparison based on the use of three fluorophores, Biochim. Biophys. Acta 985 (1989) 271–278.
[23] J.P. Slotte, Effect of sterol structure on molecular interactions and lateral domain formation in monolayers containing dipalmitoyl phosphatidylcholine, Biochim. Biophys. Acta 1237 (1995) 127–134.
[24] X.M. Li, M.M. Momsen, H.L. Brockman, R.E. Brown, Sterol structure and sphingomyelin acyl chain length modulate lateral packing elasticity and detergent solubility in model membranes, Biophys. J. 85 (2003) 3788–3801.
[25] D. Marsh, Electron spin resonance: spin labels, in: E. Grell (Ed.), Membrane Spectroscopy, Springer Verlag, Berlin, 1981, pp. 52–141.
[26] S. Berne, K. Sepčić, G. Anderluh, T. Turk, P. Maček, N. Poklar Ulrih, Effect of pH on the pore forming activity and conformational stability of ostreolysin, a lipid raft-binding protein from the edible mushroom *Pleurotus ostreatus*, Biochemistry 44 (2005) 11137–11147.
[27] M. Palmer, Cholesterol and the activity of bacterial toxins, FEMS Microbiol. Lett. 238 (2004) 281–289.
[28] L.D. Nelson, A.E. Johnson, E. London, How interaction of perfringolysin O with membranes is controlled by sterol structure, lipid structure, and physiological low pH: insights into the origin of perfringolysin O-lipid raft interaction, J. Biol. Chem. 283 (2008) 4632–4642.
[29] L.J. Pike, Lipid rafts: heterogeneity on the high seas, Biochem. J. 378 (2004) 281–292.
[30] R.F. de Almeida, L.M. Loura, A. Fedorov, M. Prieto, Lipid rafts have different sizes depending on membrane composition: a time-resolved fluorescence resonance energy transfer study, J. Mol. Biol. 346 (2005) 1109–1120.
[31] J.F. Hancock, Lipid rafts: contentious only from simplistic standpoints, Nat. Rev. Mol. Cell. Biol. 7 (2006) 456–462.
[32] K. Roper, D. Corbeil, W.B. Huttner, Retention of prominin in microvilli reveals distinct cholesterol-based lipid micro-domains in the apical plasma membrane, Nat. Cell Biol. 2 (2000) 582–592.
[33] S. Mishra, P.G. Joshi, Lipid raft heterogeneity: an enigma, J. Neurochem. 103 (2007) 135–142.
[34] Y. Chen, J. Qin, J. Cai, Z.W. Chen, Cold induces micro- and nano-scale reorganization of lipid raft markers at mounds of T-cell membrane fluctuations, PLoS ONE 4 (2009) 1–12.
[35] J. Zidar, F. Merzel, M. Hodošček, K. Rebolj, K. Sepčić, P. Maček, D. Janežič, Liquid-ordered phase formation in cholesterol/sphingomyelin bilayers: all-atom molecular dynamics simulations, J. Phys. Chem. B 113 (2009) 15795–15802.
[36] J.J. Flanagan, R.K. Tweten, A.E. Johnson, A.P. Heuck, Cholesterol exposure at the membrane surface is necessary and sufficient to trigger perfringolysin O binding, Biochemistry 28 (2009) 3977–3987.